

The BLAST Survey of the Vela Molecular Cloud: Dynamical Properties of the Dense Cores in Vela-D

Luca Olmi,^{1,2,†} Daniel Anglés-Alcázar,³ Massimo De Luca,⁴ Davide Elia,⁵ Teresa Giannini,⁶
Dario Lorenzetti,⁶ Fabrizio Massi,² Peter G. Martin,^{7,8} Francesco Strafella⁹

ABSTRACT

The Vela-D region, according to the nomenclature given by Murphy & May (1991), of the star forming complex known as the Vela Molecular Ridge (VMR), has been recently analyzed in details by Olmi (2009), who studied the physical properties of 141 pre- and proto-stellar cold dust cores, detected by the “Balloon-borne Large-Aperture Submillimeter Telescope” (BLAST) during a much larger (55 deg²) Galactic Plane survey encompassing the whole VMR. This survey’s primary goal was to identify the coldest, dense dust cores possibly associated with the earliest phases of star formation. In this work, the dynamical state of the Vela-D cores is analyzed. Comparison to dynamical masses of a sub-sample of the Vela-D cores estimated from the ¹³CO survey of Elia (2007), is complicated by the fact that the ¹³CO linewidths are likely to trace the lower density intercore material, in addition to the dense gas associated with the compact cores observed by BLAST. In fact, the total internal pressure of these cores, if estimated using the ¹³CO linewidths, appears to be higher than the cloud ambient pressure. If this were the case, then self-gravity and surface pressure would be insufficient to bind these cores and an additional source of external confinement (e.g., magnetic field pressure) would be required. However, if one attempts to scale down the ¹³CO linewidths, according to the observations of high-density tracers in a small sample of sources, then most proto-stellar cores would result effectively gravitationally bound.

Subject headings: submillimeter: ISM — stars: formation — ISM: clouds — balloons

1. INTRODUCTION

Pre-stellar cores represent a very early stage of the star formation (SF) process, before collapse results in the formation of a central protostar. The physical and dynamical properties of these cores can reveal important clues about their nature. More than a thousand new pre- and proto-stellar cores have been identified by BLAST, the Balloon-borne Large-Aperture Submillimeter Telescope (Pascale 2008), during its second long duration balloon (LDB) science flight in 2006. BLAST detected these cold cores in a ~ 50 deg² map of the Vela Molecular Ridge (VMR) (Netterfield 2009), and was capable of constraining the temperatures of the detected sources

¹University of Puerto Rico, Rio Piedras Campus, Physics Department, Box 23343, UPR station, San Juan, Puerto Rico

²Osservatorio Astrofisico di Arcetri - INAF, Largo E. Fermi 5, I-50125, Firenze, Italy.

³University of Arizona, Department of Physics, 1118 E. Fourth Street, PO Box 210081, Tucson, AZ 85721

⁴LERMA-LRA, UMR 8112 du CNRS, Observatoire de Paris, École Normale Supérieure, UPMC & UCP, 24 rue Lhomond, 75231 Paris Cedex 05, France

⁵Istituto di Fisica dello Spazio Interplanetario - INAF, via Fosso del Cavaliere 100, I-00133 Roma, Italy.

⁶Osservatorio Astronomico di Roma - INAF, Via Frascati 33, I-00040 Monteporzio Catone, Roma, Italy.

⁷Canadian Institute for Theoretical Astrophysics, University of Toronto, 60 St. George Street, Toronto, ON M5S 3H8, Canada

⁸Department of Astronomy & Astrophysics, University of Toronto, 50 St. George Street, Toronto, ON M5S 3H4, Canada

⁹Dipartimento di Fisica, Università del Salento, CP 193,

I-73100 Lecce, Italy.

[†]olmi.luca@gmail.com,olmi@arcetri.astro.it

using its three-band photometry (250, 350, and 500 μm) near the peak of the cold core SED.

The VMR (Murphy & May 1991, Liseau et al. 1992) is a giant molecular cloud complex within the galactic plane, in the area $260^\circ \lesssim l \lesssim 272^\circ$ and $-2^\circ \lesssim b \lesssim 3^\circ$, hence located outside the solar circle. Its main properties have been recently revisited by Netterfield (2009) and Olmi (2009). In particular, Olmi (2009) used both BLAST and archival data to determine the spectral energy densities (SEDs) and the physical parameters of each source detected by BLAST in the smaller region of Vela-D, where observations from IR (Giannini 2007) to millimeter wavelengths (Massi et al. 2007) were already available.

In this work we will use the spectral line data of Elia (2007) to perform an analysis of the dynamical state of the cores. In Section 2 we discuss which cores are gravitationally bound. Then in Section 3 we discuss the effects of pressure. We draw our conclusions in Section 4.

2. DYNAMICAL STATE OF THE CORES

2.1. Core Size Distribution

The cores in Vela-D have a similar range of sizes ($\langle R_c \rangle = 0.09 \pm 0.02$ pc) to those in the overall VMR ($\langle R_c \rangle = 0.07 \pm 0.02$ pc), for comparable range of masses. Please note that although we use the term core size, or core radius, what we actually measure with BLAST is an “effective core width”, set by the power-law distribution of the column density in the core and by the BLAST beam. The small range of sizes for a large range of masses in both VMR and Vela-D is similar to what Enoch et al. (2008) found for the proto-stellar cores in Serpens, Ophiucus and, to a lesser degree, in Perseus.

We also evaluated the ratios of angular deconvolved size (from BLAST) to beam size, $\theta_{\text{dec}}/\theta_{\text{mb}}$. Power-law density profiles in pre-stellar cores have received both a theoretical (see for example the discussions in Young et al. 2003 and McKee & Ostriker 2007) and observational support (e.g., Ward-Thompson et al. 1999, Andre et al. 2000 and references therein). Assuming that also the Vela-D cores can be described by power-law density profiles, then according to Young et al. (2003) $\theta_{\text{dec}}/\theta_{\text{mb}}$ should depend only on the index of the power law, and not on the distance of the source. We find $\theta_{\text{dec}}/\theta_{\text{mb}}$ to have

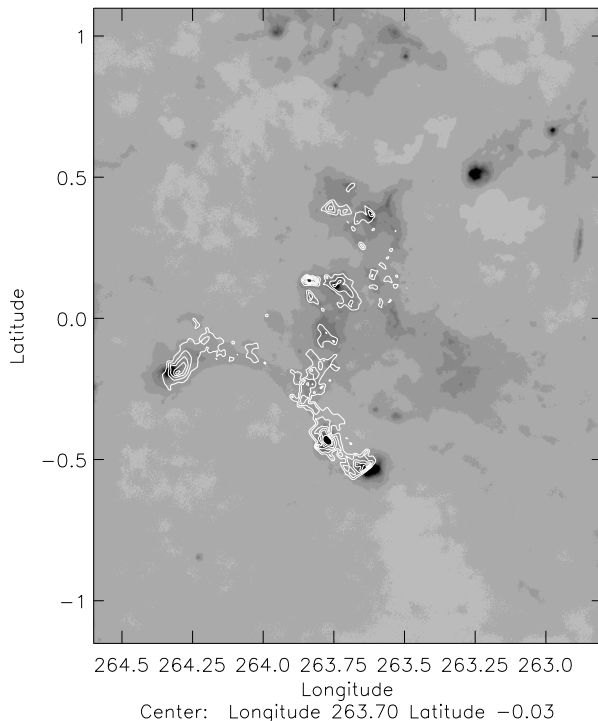


Fig. 1.— Gray-scale image shows the BLAST 250 μm map of Vela-D, with galactic coordinates in degrees. Solid contours represent the $^{13}\text{CO}(2-1)$ emission (from Elia 2007), integrated between 2 km s^{-1} and 15 km s^{-1} . The first contour is at 2 K km s^{-1} , and contour spacing is $\simeq 7 \text{ K km s}^{-1}$.

a median value of 1.41 for Vela-D, corresponding to a density power-law exponent $p \simeq 1.6$ (Young et al. 2003). This value for the power-law exponent, similar to that found by Enoch et al. (2008) in Ophiucus, is consistent with mean p -values found from radiative transfer modeling of Class 0 and Class I envelopes (Young et al. 2003).

2.2. Bonnor-Ebert Analysis

In this section we investigate the dynamical state of starless and proto-stellar cores, in order to determine whether or not the BLAST starless cores in Vela-D are pre-stellar, i.e. they will collapse and form one or more stars. We first analyze the dynamical state of the cores by calculating the critical Bonnor-Ebert mass, M_{BE} . In this analysis we assume that all cores are spherical in shape, as our angular resolution at the distance of Vela-D is not sufficient to determine with enough accuracy the ellipticity of the cores. Because elongated cores can be considerably more stable than expected from a pure spherical Bonnor-Ebert model (e.g., Stahler & Palla 2004), then we may be over-estimating the non-stability of some cores. Furthermore, it should be noted that even if the core mass is larger than the Bonnor-Ebert mass, this condition alone does not guarantee that the core is truly gravitationally unstable, as we are neglecting any other non-thermal support. Other sources of support are discussed in the next sections.

The Bonnor-Ebert mass, M_{BE} , can be determined from the observables, i.e. the core radius and temperature:

$$M_{\text{BE}}[M_{\odot}] = 1.8R_{\text{BE}}[\text{pc}]T[\text{K}] \quad (1)$$

where T is the core temperature, as determined from the SED fits (Olmi 2009), and R_{BE} represents the core radius at which the internal and ambient pressures are equal, for a Bonnor-Ebert sphere in hydrostatic equilibrium.

R_{BE} can be estimated as $R_{\text{BE}} = f R_{\text{dec}}$, where R_{dec} is the measured linear deconvolved half-width at half-maximum and f is a numerical factor that has been determined as follows. For each core the approximated Bonnor-Ebert density profile for an isothermal sphere, flat at the core center¹ and falling off with r^{-2} to the outside (see Figure 2),

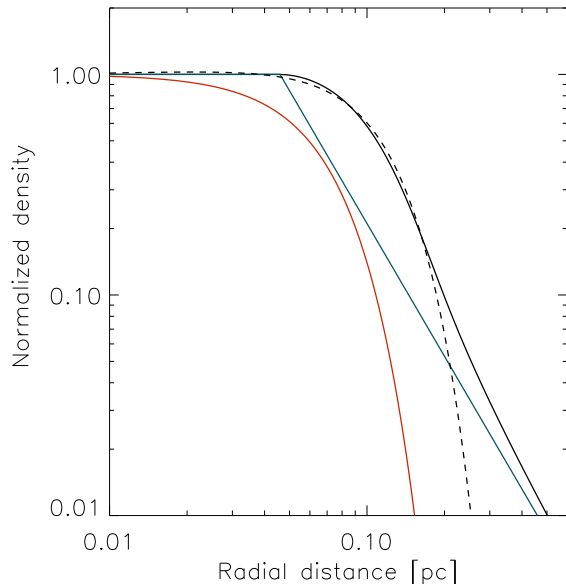


Fig. 2.— Example showing how R_{BE} is estimated. The red solid line represents the profile of the BLAST $250 \mu\text{m}$ beam at the distance of Vela-D. The blue solid line shows the approximated Bonnor-Ebert density profile, from which the simulated R_{BE} is calculated. The black solid line represents the convolution of the beam and density profiles, and the dashed black line shows the Gaussian best-fit to the convolved profile, from which the source simulated radius, R^{sim} (HWHM), is determined.

¹The core center is defined here as the region where the normalized radius $r_n < 1$, with $r_n = r \sqrt{4\pi G m_{\text{av}} \rho_0 / (kT)}$,

is generated. The density profile is obtained using the temperature and average density estimated for each core, and the theoretical radius, R_{BE} , of this sphere is estimated. This profile is then convolved with the BLAST beam at $250 \mu\text{m}$ and then fitted with a Gaussian, obtaining a simulated “observed” radius R^{sim} (defined as the half-width at half-maximum of the fitting Gaussian). Finally, this simulated radius is deconvolved, obtaining $R_{\text{dec}}^{\text{sim}}$, and then compared with R_{BE} . Their ratio is then the factor $f = R_{\text{BE}}/R_{\text{dec}}^{\text{sim}}$ specific to that source. The factor f can then be used to determine R_{BE} from the *measured* radius, R_{dec} , thus keeping into account any mismatch between $R_{\text{dec}}^{\text{sim}}$ and R_{dec} .

At the distance of Vela-D, and for the range of core temperatures found in this cloud, we find an average value $\langle f \rangle = 2.55 \pm 0.14$. Thus, from the observed R_{dec} and core temperature, the value of M_{BE} can be estimated. To further rid the sample of unrealistically small core sizes we also eliminated all data for which the beam radius exceeded the deconvolved source radius. See Jijina et al. (1999) and Enoch et al. (2007) for further discussion on the effects of instrumental resolution.

Figure 3 plots the total core mass, M_{core} , also determined from the SED fits, vs. the Bonnor-Ebert mass for all BLAST cores in Vela-D that have well-determined SED fits. We also plot the completeness limits and a vertical -dashed line corresponding to the estimated minimum measurable Bonnor-Ebert mass, calculated as;

$$M_{\text{BE}}^{\text{min}} [M_{\odot}] = 1.8 R_{\text{BE}}^{\text{min}} [\text{pc}] T_{\text{compl}} [\text{K}] \quad (2)$$

where $T_{\text{compl}} = 12 \text{ K}$, and $R_{\text{BE}}^{\text{min}} = \langle f \rangle R_{\text{beam}}$, where R_{beam} corresponds to the beam linear half-width at half-maximum at the distance of Vela-D.

The cores with $M_{\text{core}} \geq M_{\text{BE}}$ represent sources which, *in the absence of further internal support* (turbulent, magnetic, etc.), are gravitationally unstable and will collapse (or are already collapsing) in the presence of external perturbations. Without further knowledge of the internal structure of these cores we *cannot* yet establish whether they are collapsing or will collapse to form stars. On the other hand, the cores with $M_{\text{core}} < M_{\text{BE}}$ represent sources which, assuming only thermal support as in Bonnor-Ebert spheres, are *stable* against

where m_{av} is the mass of the average gas particle and ρ_0 is the density at the center of the core.

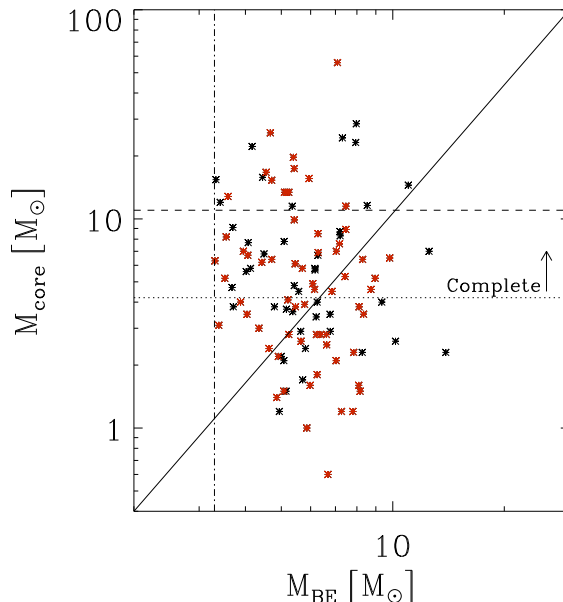


Fig. 3.— Total core mass, derived from the SED fits, vs. the Bonnor-Ebert mass. Red symbols are for starless cores, black symbols for proto-stellar cores. The median value of M_{BE} is $5.7 M_{\odot}$. The solid line corresponds to $M_{\text{core}} = M_{\text{BE}}$. The two horizontal lines correspond to the completeness limits for sources with $T > 12 \text{ K}$ (dotted line) and $T > 10 \text{ K}$ (dashed line), respectively (Olmí 2009). The vertical dot-dashed line correspond to the estimated minimum measurable Bonnor-Ebert mass, $M_{\text{BE}}^{\text{min}}$.

external perturbations. Any further internal support will thus add to their stability against gravitational collapse, and might eventually lead to the core disruption.

We find a median $M_{\text{core}}/M_{\text{BE}} = 0.9$ for all sources in Vela-D, i.e. very near the critical value, and indicating that we have about the same number of sources with $M_{\text{core}} < M_{\text{BE}}$ and $M_{\text{core}} > M_{\text{BE}}$. However, if we restrict ourselves to mass ranges for which we are progressively more complete ($M_{\text{core}} \gtrsim 4 M_{\odot}$, see Table 3 of Olmi 2009), our sources exceed their corresponding Bonnor-Ebert mass by a median factor of $M_{\text{core}}/M_{\text{BE}} = 1.5 - 3.3$. Figure 3 shows very little difference between starless and proto-stellar cores, and we can also see that the core mass range where the critical value $M_{\text{core}} = M_{\text{BE}}$ is crossed is $M_{\text{core}} \sim 3 - 8 M_{\odot}$. In this range we are only partially complete (see Netterfield 2009 and Olmi 2009) and thus more sensitive measurements are needed in order to confirm that this is an evolutionary effect.

2.3. Virial Analysis

2.3.1. Determination of Virial Masses

We now investigate the dynamical state of the Vela-D cores by estimating their virial masses. The comparison of dust-derived masses to molecular line observations gives a more robust method of determining if the cores are gravitationally bound. In fact, while our determination of the dust masses provide an estimate of the gravitational potential energy, the molecular linewidths constitute a measure of the internal energy of the cores, provided that the selected molecular lines are truly tracers of the cores observed at (sub)millimeter wavelengths. This is typically the case with molecular probes of the interior of pre- and proto-stellar cores, such as NH_3 and N_2H^+ , whereas more abundant and diffuse molecules, such as ^{13}CO described below, will provide only an upper limit to the internal energy of the cores.

Here we will be using the $^{13}\text{CO}(2-1)$ data of Elia (2007), but instead of using the catalog of these authors (obtained by CLUMPFIND, Williams et al. 1994) to associate a molecular clump to a BLAST core, we use the coordinates of the BLAST objects (when they fall within the ^{13}CO map of Elia 2007) to find the corresponding $^{13}\text{CO}(2-1)$ spectrum along the line of sight. This

procedure has two advantages: first, we avoid associating the same catalog clump (generally somewhat more massive and larger in size) to multiple BLAST cores, and in addition we can directly perform a Gaussian fit of the $^{13}\text{CO}(2-1)$ line without having to rely on the ability of CLUMPFIND to separate adjacent (in space and velocity) clumps.

We selected only BLAST cores with corresponding well-determined $^{13}\text{CO}(2-1)$ linewidths (a total of 35 sources). In the spectra of four sources we find multiple ^{13}CO velocity components along the line-of-sight to the BLAST core. However, in three of these sources we observe only two velocity components, and their linewidths are very similar or they differ by less than 50%. Thus, as long as the linewidths are not too different, it does not matter which of the two $^{13}\text{CO}(2-1)$ velocity components is actually associated with the BLAST core. In the remaining source we find multiple velocity components with linewidths ranging from 0.3 km s^{-1} to 1.8 km s^{-1} , and because we cannot know with certainty which one is actually associated with the BLAST core, we did not use it for the determination of the virial mass.

We estimate the virial mass of the cores as (MacLaren et al. 1988):

$$M_{\text{vir}}[M_{\odot}] = 210 R_{\text{dec}}[\text{pc}] (\Delta V[\text{km s}^{-1}])^2 \quad (3)$$

where ΔV represents the total linewidth of the mean particle, and is calculated as the sum of the thermal and turbulent components:

$$\Delta V^2 = \Delta V_{^{13}\text{CO}}^2 + kT8 \ln 2 \left(\frac{1}{m_{\text{av}}} - \frac{1}{m_{^{13}\text{CO}}} \right) \quad (4)$$

where $\Delta V_{^{13}\text{CO}}$ is the $^{13}\text{CO}(2-1)$ line FWHM, $m_{\text{av}} = 2.3 \text{ amu}$ is the mean molecular weight and $m_{^{13}\text{CO}} = 29 \text{ amu}$ is the molecular weight of ^{13}CO .

Figure 4 plots the total core mass M_{core} vs. the virial mass M_{vir} for all the BLAST cores in Vela-D selected as described above. The solid line in this figure represents the self-gravitating limit defined by $K = -U$, where K is the kinetic and U the gravitational potential energy, corresponding to $M_{\text{core}} = 0.5 M_{\text{vir}}$. We note that one could expand the definition of Bonnor-Ebert mass to include the effects of turbulence, thus writing Eq. (1) as:

$$M_{\text{BET}}[M_{\odot}] = 1.8 R_{\text{BE}}[\text{pc}] T_{\text{eff}}[\text{K}] \quad (5)$$

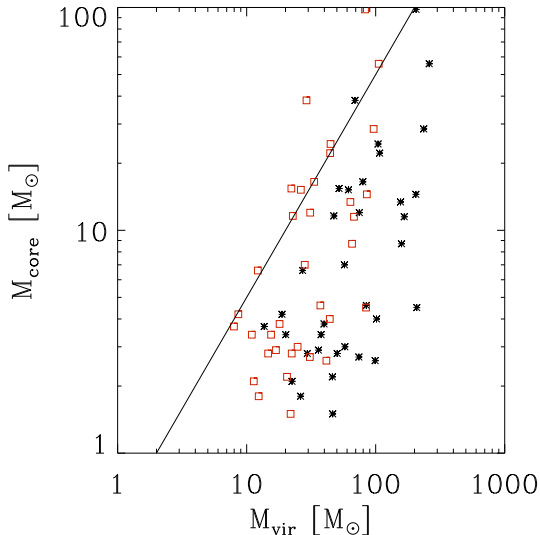


Fig. 4.— Total core mass, derived from the SED fits, vs. the virial mass, calculated using the velocity linewidth derived from the $^{13}\text{CO}(2-1)$ data of Elia (2007). The solid line indicates the minimum $M_{\text{core}} = 0.5M_{\text{vir}} = 0.5M_{\text{BET}}$ for which the cores should be self-gravitating. Black asterisks represent the results when no scale factor is applied to the $^{13}\text{CO}(2-1)$ linewidths, whereas the red open squares show the resulting parameters when the linewidths are scaled (with the 1.6 factor, see text) and thus are thought to represent more closely the core internal velocity dispersion. For the sake of simplicity, both starless and proto-stellar cores are represented by the same symbols.

where the effective temperature, T_{eff} , is defined as the temperature that describes the total line width, i.e.:

$$\Delta V^2 = \frac{kT_{\text{eff}} 8 \ln 2}{m_{\text{av}}} \quad (6)$$

which also gives $T_{\text{eff}} [\text{K}] = 50 \Delta V^2 [\text{km s}^{-1}]$. Eq. (5) then becomes:

$$M_{\text{BET}} [M_{\odot}] = 90 f R_{\text{dec}} [\text{pc}] \Delta V^2 [\text{km s}^{-1}], \quad (7)$$

where we have used $R_{\text{BE}} = f R_{\text{dec}}$ (see Section 2.2). We therefore see that $M_{\text{BET}} \simeq M_{\text{vir}}$, and the self-gravitating limit corresponds to $M_{\text{core}} = 0.5 M_{\text{vir}} \simeq 0.5 M_{\text{BET}}$.

In Figure 4 we can see that nearly all of the cores lie below the self-gravitating line, indicating that they are unlikely to be gravitationally bound, in agreement with the findings of Elia (2007) and Massi et al. (2007). However, the $^{13}\text{CO}(2-1)$ emission may be partially optically thick along the line of sight of the ^{13}CO clump centroid (see Elia 2007), and even when it is indeed optically thin it traces all molecular gas along the line of sight. Although, as we discussed earlier, we measure the ^{13}CO linewidths along the line of sight to the BLAST cores and not toward the clumps centroid of Elia (2007), we are likely to trace the lower density intercore material in addition to the dense gas associated with the compact cores observed by BLAST. We attempt to correct for this effect in the next section.

2.3.2. Application of a Scaling Factor for the Linewidths

Recent follow-up observations toward a sample of the Vela-D cores (Olmli et al., *in preparation*) have allowed us to determine the average of the $^{13}\text{CO}(2-1)$ to $\text{N}_2\text{H}^+(1-0)$ linewidth ratio, equal to $\simeq 1.6$, in a small sub-sample of 7 cores. For comparison, in the Pipe cores Rathborne et al. (2008) find that the C^{18}O linewidths, in the range $\sim 0.14 - 0.61 \text{ km s}^{-1}$ (Muench et al. 2007), are typically 1.4 times broader than NH_3 which, like N_2H^+ , traces only the gas associated with the dense compact core. Furthermore, Onishi (1999) found that the ^{13}CO emission lines from the Pipe cloud were characterized by linewidths of $\sim 1 \text{ km s}^{-1}$. This leads in this case to a typical ^{13}CO to NH_3 linewidth ratio of $\simeq 2.8$.

The difference between the two scale factors may be caused, besides to the statistical significance of the two samples of sources, also by real dynamical differences between the Vela-D and Pipe regions. In fact, both Elia (2007) and Massi et al. (2007) find evidence for turbulent activity in Vela-D. In addition, the presence of multiple IRAS embedded clusters, stellar jets and outflows also suggest that overall Vela-D is in a more advanced evolutionary state compared to the Pipe nebula.

We also note that if we use the NH_3 survey of Jijina et al. (1999) and the ^{13}CO survey of Vilas-Boas et al. (2000), the average ^{13}CO to NH_3 linewidth ratios toward, e.g., the Ophiucus and Taurus clouds would be even larger than that estimated for the Pipe cores. Therefore, the reader should consider the results obtained by applying the linewidth scale factors with caution. In the following, we will use the 1.6 scale factor obtained toward Vela-D as our baseline value, but we will occasionally discuss how the results would change if a larger (typical of other clouds) scale factor were used.

2.3.3. Comparison with Previous Results

Comparing Figures 3 and 4 we note that the core mass, $M_{\text{core}} \simeq 3 - 8 M_{\odot}$, at which the critical threshold $M_{\text{core}} = M_{\text{BE}}$ is crossed, is quite lower than the mass at which the cores appear to become gravitationally bound, which from Figure 4 can be roughly estimated to be $\gtrsim 30 M_{\odot}$, when the scale factor for the linewidths is applied. Looking at Figure 12 of Olmi (2009), it would be tempting to infer that the characteristic mass at which the core mass function appears to break or depart from a power-law is similar with the critical Bonnor-Ebert mass of Figure 3. However, we cannot compare these mass ranges because of the completeness limit. Thus, we cannot confirm for Vela-D the results obtained by Lada et al. (2008) for the Pipe cores, where the authors find a consistency between all of these critical mass ranges.

As far as the results of Elia (2007) are concerned, we have already seen that we associate a BLAST core to a single $^{13}\text{CO}(2-1)$ velocity component, whereas in the clump catalog of Elia (2007) multiple gas clumps may be associated with a group of dust cores, as detected by Massi et al. (2007). Because of this and also be-

cause Elia (2007) do not attempt to correct the $^{13}\text{CO}(2-1)$ linewidths, it is not surprising that their virial masses turn out to be a factor $\sim 3-40$ larger than the estimated gas mass of each clump.

On the other hand, assuming that either N_2H^+ or NH_3 trace the bulk of the core emission, one can apply the 1.6 scale factor estimated in Section 2.3.2 to the $^{13}\text{CO}(2-1)$ linewidths. In this case we find that $\simeq 35\%$ of the Vela-D cores detected by BLAST within the area covered by the $^{13}\text{CO}(2-1)$ map of Elia (2007) are near or over the threshold to become gravitationally bound, as shown in Figure 4. If we had used a larger linewidth scale factor, such as the one derived from the Pipe cores, nearly half of the Vela-D cores would result gravitationally bound, according to this analysis. However, the exact fraction of bound cores will be known only when the linewidth of each core will be individually measured with a high-density tracer.

3. EFFECTS OF PRESSURE

3.1. Cores Edge Pressure

To further investigate the dynamical state of the Vela-D cores we now analyze the effects of thermal and non-thermal pressures on the cores. First, we compare the core mass with the estimated radius of the Bonnor-Ebert sphere, for a given edge pressure. The Bonnor-Ebert critical mass can be written in terms of its radius and of the pressure, P_{\circ} , at the edge of the sphere (equal to the ambient pressure) as:

$$M_{\text{BE}}[M_{\odot}] = 0.15 (D_{\text{BE}}[\text{pc}])^2 (P_{\circ}/k[\text{cm}^{-3} \text{K}])^{1/2}. \quad (8)$$

In the top panel of Figure 5 we have thus plotted for each core where a measurement of M_{vir} was available, the edge pressure P_{\circ}/k , corresponding to a Bonnor-Ebert sphere (with given radius and temperature) in hydrostatic equilibrium, as a function of the $M_{\text{core}}/M_{\text{BE}}$ ratio. In addition, we have also plotted the sources where $M_{\text{core}}/M_{\text{vir}} \geq 0.5$.

Given the small number of data points, the interpretation of the top panel of Figure 5 is difficult. The number of data points becomes even smaller if we take into account the fact that the definition of P_{\circ} is only valid for sources *at or near the Bonnor-Ebert equilibrium*. For this reason we

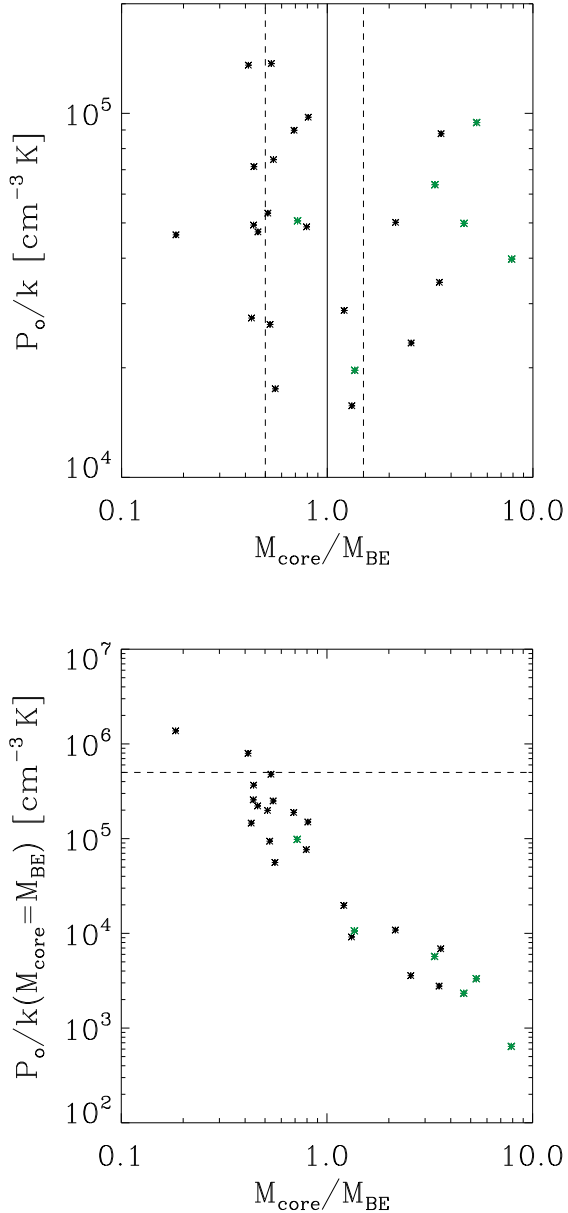


Fig. 5.— *Top*. Pressure, P_o/k , at the edge of the Bonnor-Ebert sphere (equal to the ambient pressure) vs. $M_{\text{core}}/M_{\text{BE}}$, for all points where a virial mass could be determined. The green symbols represent cores with $M_{\text{core}} \geq 0.5 M_{\text{vir}}$ (1.6 scale factor applied, see text); black symbols are for cores with $M_{\text{core}} < 0.5 M_{\text{vir}}$. *Bottom*. Edge pressure calculated assuming $M_{\text{BE}} = M_{\text{core}}$ (see text). Green and black symbols are as before. The dashed horizontal line corresponds to the ambient pressure in Vela-D, $P_{\text{ext}}/k \sim 5 \times 10^5 \text{ cm}^{-3} \text{ K}$ (see Section 3.2).

have drawn in Figure 5 two dashed vertical lines corresponding to $M_{\text{core}}/M_{\text{BE}} = 0.5, 2$ which enclose all sources having a mass within a factor of 2 from the corresponding Bonnor-Ebert mass required to be in hydrostatic equilibrium. For these points there is a wide distribution of P_o/k values, from $P_o/k \sim 10^4 \text{ cm}^{-3} \text{ K}$ to $\sim 10^5 \text{ cm}^{-3} \text{ K}$. However, we tentatively note that most sources with $M_{\text{core}}/M_{\text{BE}} < 1$ have a *higher* ($\gtrsim 4 \times 10^4 \text{ cm}^{-3} \text{ K}$) value of the edge pressure, compared to those objects with $M_{\text{core}}/M_{\text{BE}} > 1$ (three sources only, with pressure $\lesssim 3 \times 10^4 \text{ cm}^{-3} \text{ K}$). This is indeed what one might expect in cores with low density-contrast which are mainly confined by the external pressure, and not by self-gravity. Clearly, a larger source sample is needed to confirm that this trend is real. We also note that most sources with $M_{\text{core}}/M_{\text{vir}} \geq 0.5$ (with a 1.6 scale factor) also have $M_{\text{core}}/M_{\text{BE}} > 1$, a trend which is confirmed when a larger linewidth scale factor is used.

In the bottom panel of Figure 5 we have instead plotted the edge pressure, P_o/k , assuming $M_{\text{BE}} = M_{\text{core}}$, as a function of the $M_{\text{core}}/M_{\text{BE}}$ ratio, estimated as described in Section 2.2. From Equations (1) and (8) one can see that $P_o/k \propto T^4 M_{\text{BE}}^{-2}$. Therefore, for cores with $M_{\text{core}}/M_{\text{BE}} < 1$, the edge pressure calculated as $P_o/k \propto T^4 M_{\text{core}}^{-2}$ represents the *external* pressure required to make the core gravitationally *unstable*. On the other hand, in the cores where $M_{\text{core}}/M_{\text{BE}} > 1$ the quantity $P_o/k \propto T^4 M_{\text{core}}^{-2}$ represents the *internal* pressure required to make the core *stable* against gravitational collapse.

Since the ambient pressure in the densest parts of the Vela-D region has been estimated to be $P_{\text{ext}}/k \sim 5 \times 10^5 \text{ cm}^{-3} \text{ K}$ (see Section 3.2) the bottom panel of Figure 5 is suggesting that the cores with $M_{\text{core}}/M_{\text{BE}} < 1$ are actually likely to undergo gravitational collapse at some point in the future, unless an additional, non-thermal source of internal support exist. This internal support could in fact be of turbulent origin, since most of the points with $M_{\text{core}}/M_{\text{BE}} < 1$ also have $M_{\text{core}}/M_{\text{vir}} < 0.5$ (see Section 2.3).

On the other hand, the cores with $M_{\text{core}}/M_{\text{BE}} > 1$ show that the required internal, thermal pressure to remain in equilibrium is much less than the ambient pressure in Vela-D. Thus, these cores are also likely to undergo gravitational collapse, except possibly the objects with $M_{\text{core}}/M_{\text{vir}} < 0.5$,

which have an additional source of internal turbulent support.

3.2. Thermal and non-Thermal Pressure

We now specifically consider the ratio of thermal to non-thermal pressure, $R_p = (a/\sigma_{\text{NT}})^2$, for each core; here $a = [kT/(\mu \text{amu})]$ is the one-dimensional isothermal sound speed in the gas, $\sigma_{\text{NT}} = \Delta V_{\text{NT}}/(8 \log 2)^{1/2}$ represents the non-thermal component of the velocity dispersion, and $\Delta V_{\text{NT}} = [\Delta V_{\text{13CO}}^2 - 8 \log 2 kT/m_{\text{13CO}}]^{1/2}$, where ΔV_{13CO} is the observed linewidth.

In the top panel of Figure 6 we plot R_p vs. core mass with and without the scale factor for the linewidths (Section 2.3). This figure shows that all of the cores in Vela-D for which we have a measured $\text{13CO}(2-1)$ linewidth are below the $R_p = 1$ line, and thus the non-thermal pressure would appear to exceed the thermal pressure. Figure 6 also shows that the situation only marginally change if the linewidths are scaled with the 1.6 factor. Many more cores would have $R_p > 1$ if the larger 2.8 scale factor from the Pipe cores were used. In fact, Lada et al. (2008) found in the Pipe cores that where both NH_3 and C^{18}O are observed, the non-thermal pressure derived from the C^{18}O data is on average a factor of 4 larger than that measured by the ammonia line.

We then evaluate the *average* total internal pressure of each core in Vela-D for which we have measured the $\text{13CO}(2-1)$ linewidth. We note that this pressure will overestimate the pressure at the edge of the cores. Including both thermal and non-thermal contributions, the pressure is given by:

$$P_{\text{tot}} = \rho (a^2 + \sigma_{\text{NT}}^2) \quad (9)$$

where ρ is the mean density of a core. In the bottom panel of Figure 6 we plot the quantity P_{tot}/k vs. core mass, where we note the high values of the pressure, due to the relatively high density of the cores and to the large $\text{13CO}(2-1)$ linewidths. These values are consistent with the cores internal pressure estimated by Massi et al. (2007), who also found that the external pressure to the cores is of order $P_{\text{ext}}/k \sim 5 \times 10^5 \text{ cm}^{-3} \text{ K}$. However, if the 1.6 scale factor for the linewidths is applied, the total internal pressure would vary, for most cores (Figure 6), in the range $P_{\text{tot}}/k \sim 5 \times 10^5 - 4 \times 10^7 \text{ cm}^{-3} \text{ K}$, comparable to the ambient pressures characterizing other SF regions.

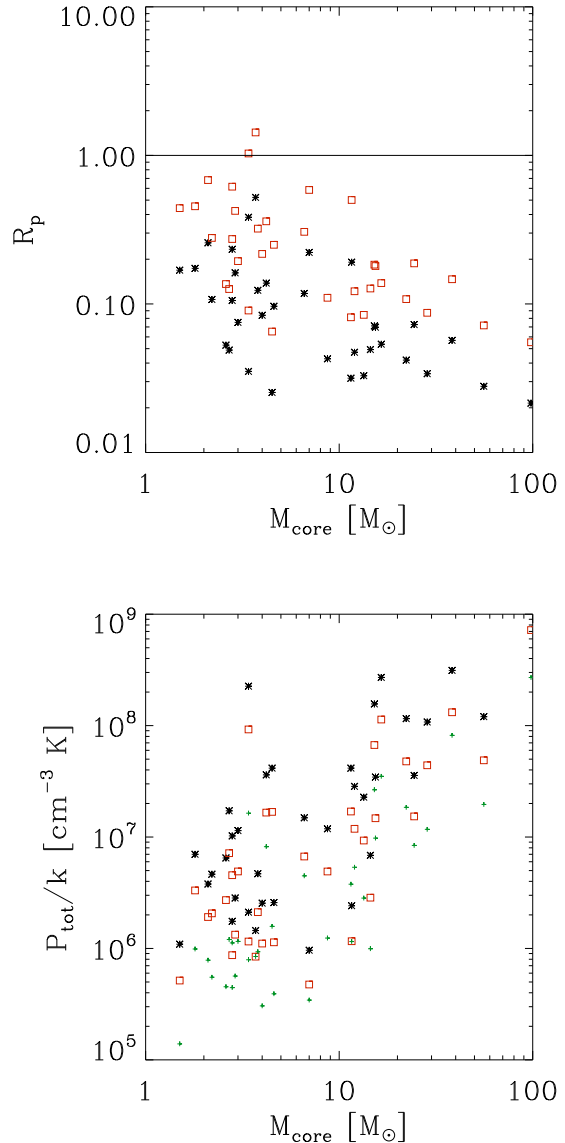


Fig. 6.— *Top*. Ratio of thermal to non-thermal pressure for the Vela-D cores vs. core mass. *Bottom*. Total core internal gas pressure plotted as a function of core mass. Symbols are as in Figure 4. The small green “+” signs correspond to the pressure calculated using a Larson-type scaling law (see text).

In the lower panel of Figure 6 it is also evident the trend of increasing P_{tot}/k for more massive cores. We find a trend of increasing density with increasing core mass in Vela-D, but this trend is not enough to explain the increase in P_{tot}/k with core mass over more than two orders of magnitude, as shown in Figure 6. Therefore, the higher value of P_{tot}/k in more massive cores must also be a consequence of the increased thermal and non-thermal components of the internal pressure. In particular, the top panel of Figure 6 shows that the contribution of the non-thermal pressure becomes dominant for high-mass cores.

This is in fact consistent with the trend observed between pressure and mass when a simple scaling law (Larson 1981) is used between the line width and the density, $\Delta V \propto \rho^{-1/2}$. According to Adams & Fatuzzo (1996) this implies a scaling relation between the linewidth and the mass of the core, which can be written as:

$$M_{\text{core}}[M_{\odot}] \simeq 466.5 (a_{\text{eff}}[\text{km s}^{-1}])^4 \quad (10)$$

this relation can also be written using Eq. (9) for the “effective” sound speed, $a_{\text{eff}}^2 = P_{\text{tot}}/\rho$, as:

$$P_{\text{tot}}[\text{dyne cm}^{-2}] = 4.6 \cdot 10^8 \rho[\text{g cm}^{-3}] (M_{\text{core}}[M_{\odot}])^{1/2} \quad (11)$$

which is plotted in the lower panel of Figure 6, in the usual units of P_{tot}/k . We note that the model pressure reproduces the trend followed by the data points, but for each specific point the pressure given by Eq. (11) generally underestimates the pressure given by Eq. (9), though to a lesser extent when the scale factor for the linewidths is applied.

3.3. What Supports the Vela-D Cores?

We thus have two possible scenarios regarding the dynamical state of the Vela-D cores, if we consider the sub-sample of cores within the area covered by the $^{13}\text{CO}(2-1)$ map as a representative sample of the whole Vela-D. If we do *not* apply the scale factor for the linewidths, then almost all of the cores would appear to be gravitationally *unbound* (Figure 4) and would have an internal pressure much higher than the core external pressure (Figure 6). We note, however, that the average value of the core deconvolved radius to sound speed ratio is $\langle R_{\text{dec}}/a \rangle = (3.2 \pm 1.1) \times 10^5 \text{ yr}$, thus quite lower compared to the estimated dynamical age, ~ 1 to $2 \times 10^6 \text{ yr}$, of the filaments and stellar

clusters in the Vela-D region (see Elia 2007 and Massi et al. 2010). This would suggest that either the gravitationally unbound cores are really transient structures (e.g., produced by the turbulence of the Vela-D region; see Elia 2007 and Massi et al. 2007) and are thus constantly replenished, or they are externally supported.

As for the latter case, Figure 6 shows that many of these cores cannot be pressure-confined. Then the question arises of how the gravitationally unbound cores can be effectively confined against their own internal pressure to still form coherent structures. Because in this case self-gravity and surface pressure alone appear to be insufficient to bind the cores, a plausible source of external confinement could come from the presence of static, helical magnetic fields within the filaments or clumps where the dense cores have formed (see Fiege & Pudritz 2000).

We can estimate the magnitude of the field strengths needed to produce the external magnetic pressure which would add to the ambient gas pressure to compensate the cores internal pressure, i.e. $P_B = B^2/(8\pi) = P_{\text{tot}} - P_{\text{ext}}$. In this way we find that the required B would vary from a few tens to several hundreds of μG . While these values are in agreement with measured magnitudes of B in molecular clouds (see, e.g., Basu 2004 and references therein), we would have to assume that all of this field is toroidal and constitutes the dominant component (Fiege & Pudritz 2000).

On the other hand, we know that the $^{13}\text{CO}(2-1)$ linewidths are indeed overestimating the core internal velocity dispersion, as discussed in the previous sections. Thus, if we do apply the approximate scale factor discussed in Section 2.3 then $\sim 30 - 50\%$ (depending on the scale factor assumed) of the cores (mostly proto-stellar) would become gravitationally bound. The internal pressure of these cores still appears to be significantly higher than the pressure of the ambient medium, but because the cores would be confined by self-gravity the high surface pressures are of no concern for the overall long-term stability of the cores.

The cores that are *not* gravitationally bound, and with internal pressures higher than the surface pressure, would still need a source of external confinement, unless they are transient structures, as discussed earlier. However, we find that many ($\simeq 40\%$) of these unbound cores (both starless

and proto-stellar) would have an internal pressure $P_{\text{tot}}/k \lesssim 2 \times 10^6$, which is a factor of 4 higher than the estimated average external pressure in Vela-D, $P_{\text{ext}}/k \sim 5 \times 10^5 \text{ cm}^{-3} \text{ K}$ (Massi et al. 2007), thus partially reducing the imbalance between internal and external pressures.

4. SUMMARY AND CONCLUSIONS

In this paper we have analyzed the dynamical state of the population of the dense and cold cores detected by BLAST in the Vela-D molecular cloud, utilizing the sensitive maps at 250, 350 and 500 μm obtained by BLAST during its 2006 LDB flight from Antarctica. We can summarize the results of this paper as follows, although some of our conclusions are still dependent on an exact measurement of the internal velocity dispersion of the cores:

1. The median $M_{\text{core}}/M_{\text{BE}} = 0.9$ for all sources in Vela-D, i.e. very near the critical value, assuming thermal support only. If we restrict ourselves to mass ranges for which we are progressively more complete, our sources exceed their Bonnor-Ebert mass by a median factor of $M_{\text{core}}/M_{\text{BE}} = 1.5 - 3.3$.

2. If the BLAST cores were purely isothermal structures, then almost all would be either confined by the external gas pressure, or by their gravity. According to the virial analysis of the cores with an unambiguous line-of-sight $^{13}\text{CO}(2-1)$ spectrum, almost none of them would appear to be gravitationally bound and would also be dominated by non-thermal pressure. However, we think this is likely a consequence of the $^{13}\text{CO}(2-1)$ linewidths overestimating the core internal velocity dispersion. Despite the uncertainties involved in this procedure, we have attempted to correct for this effect and found that $\sim 30 - 50\%$ of the cores would then turn out to be gravitationally bound.

3. The average total internal pressure of the cores appear to be higher than the ambient external pressure. If most cores were indeed gravitationally *unbound* then self-gravity and surface pressure would be insufficient to bind the cores and form coherent structures. After application of the scale factor to the $^{13}\text{CO}(2-1)$ linewidths, a significant fraction of the cores (mostly proto-stellar) would actually become gravitationally bound, and thus they would not need to be pressure-confined.

4. The cores that result gravitationally un-

bound even after application of the scale factor to the $^{13}\text{CO}(2-1)$ linewidths, would still need an additional source of external confinement. If the confinement mechanism were an external magnetic pressure, the required B would vary from a few tens to several hundreds of μG . Measurements of the BLAST cores velocity dispersion is necessary to allow a more accurate dynamical analysis.

5. Alternatively, the gravitationally unbound cores could be transient structures, continuously produced in the region by turbulence.

We acknowledge the support of NASA through grant numbers NAG5-12785, NAG5-13301, and NNGO-6GI11G, the NSF Office of Polar Programs, the Canadian Space Agency, the Natural Sciences and Engineering Research Council (NSERC) of Canada, and the UK Science and Technology Facilities Council (STFC). Support for this work was provided by NASA through an award issued by JPL/Caltech

REFERENCES

- Adams, F. C. & Fatuzzo, M. 1996, ApJ, 464, 256
- Andre, P., Ward-Thompson, D., & Barsony, M. 2000, Protostars and Planets IV, 59
- Basu, S. 2004, in Young Local Universe, Proceedings of XXXIXth Rencontres de Moriond, ed. A. Chalabaev, T. Fukui, T. Montmerle, & J. Tran-Thanh-Van
- Elia, D. *et al.* 2007, ApJ, 655, 316
- Enoch, M. L., Evans, II, N. J., Sargent, A. I., Glenn, J., Rosolowsky, E., & Myers, P. 2008, ApJ, 684, 1240
- Enoch, M. L., Glenn, J., Evans, II, N. J., Sargent, A. I., Young, K. E., & Huard, T. L. 2007, ApJ, 666, 982
- Fiege, J. D. & Pudritz, R. E. 2000, MNRAS, 311, 85
- Giannini, T. *et al.* 2007, ApJ, 671, 470
- Jijina, J., Myers, P. C., & Adams, F. C. 1999, ApJS, 125, 161
- Lada, C. J., Muench, A. A., Rathborne, J., Alves, J. F., & Lombardi, M. 2008, ApJ, 672, 410

- Larson, R. B. 1981, MNRAS, 194, 809
- Liseau, R., Lorenzetti, D., Nisini, B., Spinoglio, L., & Moneti, A. 1992, A&A, 265, 577
- MacLaren, I., Richardson, K. M., & Wolfendale, A. W. 1988, ApJ, 333, 821
- Massi, F., De Luca, M., Elia, D., Giannini, T., Lorenzetti, D., & Nisini, B. 2007, A&A, 466, 1013
- Massi, F., di Carlo, E., Codella, C., Testi, L., Vanzì, L., & Gomes, J. I. 2010, A&A, 516
- McKee, C. F. & Ostriker, E. C. 2007, ARA&A, 45, 565
- Muench, A. A., Lada, C. J., Rathborne, J. M., Alves, J. F., & Lombardi, M. 2007, ApJ, 671, 1820
- Murphy, D. C. & May, J. 1991, A&A, 247, 202
- Netterfield, C. B. *et al.* 2009, ApJ, 707, 1824
- Olmi, L. *et al.* 2009, ApJ, 707, 1836
- Onishi, T. *et al.* 1999, PASJ, 51, 871
- Pascale, E. *et al.* 2008, ApJ, 681, 400
- Stahler, S. W. & Palla, F. 2004, in The Formation of Stars, ed. WILEY-VCH
- Vilas-Boas, J. W. S., Myers, P. C., & Fuller, G. A. 2000, ApJ, 532, 1038
- Ward-Thompson, D., Motte, F., & André, P. 1999, MNRAS, 305, 143
- Williams, J. P., de Geus, E. J., & Blitz, L. 1994, ApJ, 428, 693
- Young, C., Shirley, Y., Evans, N. I., & Rawlings, J. 2003, ApJ, 145, 111